Global and multi-scale features of solar wind-magnetosphere coupling: From modeling to forecasting

A. Y. Ukhorskiy,[1] M. I. Sitnov,[2] A. S. Sharma,[2] and K. Papadopoulos[2]

Received 27 October 2003; revised 8 March 2004; accepted 17 March 2004; published 16 April 2004.

[1] The Earth's magnetosphere is a spatially extended nonlinear system driven far from equilibrium by the turbulent solar wind. During substorms it exhibits both global and multi-scale features which reconciliation has been a long standing issue. This paper presents a data-derived model of the solar wind-magnetosphere coupling that combines a nonlinear dynamical description of the global features with a statistical description of the multi-scale aspects. This approach yields deterministic predictions of the global component of magnetospheric dynamics and probabilistic predictions of its multi-scale features. *INDEX TERMS:* 2788 Magnetospheric Physics: Storms and substorms; 2784 Magnetospheric Physics: Solar wind/magnetosphere interactions; 3210 Mathematical Geophysics: Modeling; 3220 Mathematical Geophysics: Nonlinear dynamics; 3240 Mathematical Geophysics: Chaos. **Citation:** Ukhorskiy, A. Y., M. I. Sitnov, A. S. Sharma, and K. Papadopoulos (2004), Global and multi-scale features of solar wind-magnetosphere coupling: From modeling to forecasting, *Geophys. Res. Lett.*, *31*, L08802, doi:10.1029/2003GL018932.

1. Introduction

[2] The coupling of the solar wind mass, momentum and energy to the magnetosphere is the main driver of geomagnetic activity observed on the Earth and in space. The southward turning of the interplanetary magnetic field (IMF) leads to the accumulation of magnetic energy in the magnetotail which is subsequently released in the explosive process known as magnetospheric substorm. The substorms are episodic in nature and have time scales of an hour or so, and are associated with global reconfiguration of the magnetosphere. Substorms also exhibit phenomena on smaller spatial and temporal scales, such as turbulence, bursty bulk flows [*Angelopolous et. al.*, 1999], and fluctuations in the near-Earth current sheet [*Ohtani et al.*, 1995] and auroral luminosity [*Lui et al.*, 2000]. The substorm activity is often quantified with the *AL* index, which measures the magnetic field disturbances produced by the substorm current system closing through the ionosphere.

[3] Due to the wide range of spatial and temporal scales involved in the solar wind-magnetosphere interaction, developing first principles models that encompass all the relevant scales has been a challenge. Recognizing the capability of nonlinear dynamical techniques to reconstruct behavior of the system independent of modeling assumptions, long time series data of geomagnetic indices have been used to develop models in terms of a small number of dynamical variables and these have led to space weather forecasting tools based on local-linear filters [*Vassiliadis et al.*, 1995]. However, the low-dimensional models do not describe all aspects of magnetospheric dynamics. In particular, it was noted that the correlation dimension of the magnetosphere as a dynamical system does not converge on small scales. Moreover, the geomagnetic indices are found to exhibit multi-scale properties more similar to bicolored noise than to the time series generated by a low-dimensional chaotic system [*Takalo et al.*, 1994].

[4] The multi-scale properties of magnetospheric dynamics have been interpreted in terms of multi fractal behavior of intermittent turbulence and self-organized criticality [*Consolini*, 1997], motivated by the observed power-law behavior [*Tsurutani et al.*, 1990]. However, a state of self-organized criticality corresponds to the limit of vanishingly small control parameters [*Vespignani and Zapperi*, 1998], thus making the system effectively autonomous and thus questioning the validity of such models to the magnetosphere, whose dynamics is, to a large degree, driven by the solar wind. An analysis of observational data indicates that its dynamics resemble non equilibrium phase transitions [*Sitnov et al.*, 2000]. In particular, it was shown that the large-scale features of solar wind-magnetosphere coupling are organized in a manner similar to first order phase transitions. It was also suggested that the scale-free properties of the data result from the dynamics in the vicinity of a critical point, as in second order phase transitions, and a critical exponent relating the output fluctuations to the solar wind input was obtained in a form similar to the critical exponent β [*Sitnov et al.*, 2001]. The phase transition analogy provides a conceptual framework for combining the global and multi-scale aspects of substorm dynamics in a unified model. In this paper the development of such a model directly from data by combining nonlinear dynamical techniques with the conditional probability approach is presented. The solar wind convective electric field given by the product vB_S of the solar wind speed v and the southward IMF component B_S is the input of the model. The magnetospheric response to the solar wind activity is represented by the *AL* index. The model yields accurate predictions of the average level of *AL* and also ranks the probabilities of the discrepancy between the observed and predicted values of *AL*.

2. Combined Description of Global and Multi-Scale Features

[5] The model parameters are derived from the data set comprised by 34 isolated intervals representing different

[1]Applied Physics Laboratory, Johns Hopkins University, Laurel, Maryland, USA.
[2]Department of Astronomy, University of Maryland, College Park, Maryland, USA.

0094-8276/04/2003GL018932$05.00

levels of geomagnetic activity. It contains about 4×10^4 points sampled at 2.5 min intervals [*Bargatze et al.*, 1985]. In order to use both vB_S and AL data in a joint input-output phase space their time series are normalized by the respective standard deviations: $I_t = vB_S(t)/\sigma_{vB_S}$ and $O_t = AL(t)/\sigma_{AL}$ ($\sigma_{vB_S} = 976 \times$ nT km/s, $\sigma_{AL} = 171$ nT).

[6] To reconstruct the phase space underling the observed scalar time series we use the delay embedding technique developed for nonlinear dynamical systems [*Casdagli*, 1992]. The set of delay vectors given by

$$\left(\mathbf{I}_t^T, \mathbf{O}_t^T\right) = \left(I_t, \ldots, I_{t-(M-1)}, O_t, \ldots, O_{t-(M-1)}\right) \quad (1)$$

where M is the total number of delays, yields the trajectory of the system in the reconstructed space where the directions of the largest variances reveal the dominant dynamical variables. These directions are derived from a principal component analysis [*Broomhead and King*, 1986] and the dominant variables of the solar wind-magnetosphere coupling are obtained by projecting the input-output delay vectors on the first D principal components ($\mathbf{v}_1, \ldots, \mathbf{v}_D$) of $vB_S - AL$ time series as

$$\mathbf{x}_t = \left(\mathbf{I}_t^T, \mathbf{O}_t^T\right) \cdot (\mathbf{v}_1, \ldots, \mathbf{v}_D) \quad (2)$$

The multi-scale properties of $vB_S - AL$ time series have different origins compared to those of low-dimensional chaotic systems, such as the Lorenz system, in which the scale-invariance is due to the fractal nature of its attractor. The magnetosphere exhibits a wide range of scales with properties of high dimensional colored noise, presumably related to the scale-invariance of its solar wind driver [*Ukhorskiy et al.*, 2003]. This leads to complicated trajectories in the phase space on shorter scales, and as a result, a deterministic model alone does not provide an adequate description of the system [*Ukhorskiy et al.*, 2002].

[7] To reveal the global dynamics in the presence of multi-scale features an approach similar to the mean-field models in statistical physics is used. It was developed as the generalization of the false nearest neighbors technique of *Kennel et al.* [1992] for the case of stochastic dynamical systems [see *Ukhorskiy et al.*, 2003]. In this approach the evolution of the system at time t is determined by the evolution of the fixed number NN of its nearest neighbors, viz. the states that are closest to it as measured by the distance in the reconstructed space. These nearest neighbors are used to compute the center of mass $\mathbf{x}_t^{cm}$ as their average and the state of the system at the next time step is then written as a function of the center of mass:

$$O_{t+1}^{mf} = F\left(\mathbf{x}_t^{cm}\right) = \langle O_{k+1} \rangle, \mathbf{x}_k \in NN \quad (3)$$

However, in the case of many multi-scale systems, the averaging procedure may not be well defined for chosen values of the dimension and the number of nearest neighbors. Thus the model requires an additional criterion

$$if \parallel \mathbf{x}_k^{cm} - \mathbf{x}_n^{cm} \parallel \to 0 \; then \; |O_{k+1}^{mf} - O_{n+1}^{mf}| \to 0, \quad (4)$$

which ensures that the mean-field function F is well defined for the given pair of parameters (D, NN). Then, for a given

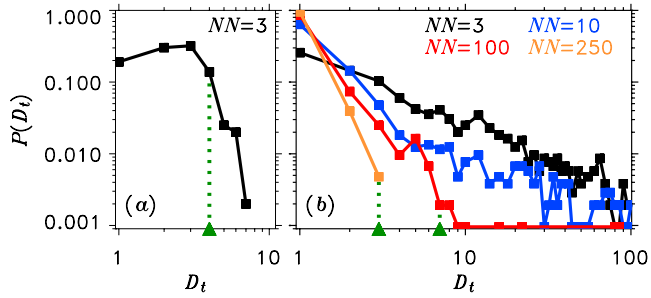

Figure 1. MFD analysis. The probability density functions of local dimension calculated with $\varepsilon = 0.1$. (a) Lorenz attractor; $D = 4$ for $NN \geq 3$ (b) $vB_S - AL$ time series; $D = 8$ for $NN = 100$, and $D = 3$ for $NN = 250$.

NN and the accuracy ε, a local minimum dimension D_t is computed such that the condition $|O_{t+1}^{mf} - \tilde{O}_{t+1}^{mf}| < \varepsilon$ holds for each point of the data set, where $\tilde{O}_{t+1}^{mf}$ is calculated with including the current state at time t in the set of nearest neighbors. The distribution of D_t is then calculated for different embedding dimensions. If for a chosen value of NN the mean-field function is well defined in some finite dimension, the distribution function drops suddenly at this value. In the absence of such a characteristic behavior NN is increased and the whole procedure is repeated. For different values of parameters (D, NN) the dynamical model (equation (3)) is computed to obtain the optimal pair of values corresponding to the highest accuracy. This value of D represents the dimension of the space with the averaging defined by NN and is referred to as the mean-field dimension (MFD).

[8] To elucidate the MFD analysis in the case of solar wind-magnetosphere system the case of Lorenz attractor, a well known low dimensional dynamical system, is studied. Figure 1a shows probability density function $P(D_t)$ calculated for the x-component of Lorenz attractor with $\varepsilon = 0.1$. Function $P(D_t)$ calculated with $NN = 3$ drops abruptly at $D_t \sim 3-4$, indicating that the ensemble averaging is well defined and that any $D \geq 4$ is a good choice for the embedding space dimension. On the other hand in case of $vB_S - AL$ time series, $P(D_t)$ calculated with small level of averaging ($NN = 3-10$) with $\varepsilon = 0.1$ have a power-law shape in $D_t = 1-100$ range (Figure 1b). This indicates that the ensemble averaging is ill defined for this range of parameters and the mean-field model is not meaningful. For increased levels of averaging ($NN \geq 100$) the functions $P(D_t)$ drop abruptly at finite values. However, unlike the Lorenz attractor which exhibits the same dimension at all scales, in the case of coupled solar wind-magnetosphere system the dimension is a function of the level of averaging. The higher the value of NN the wider the range of scales which are smoothed away and the smaller the effective dimension D of the averaged system, e.g., $D = 8$ for $NN = 100$, and $D = 3$ for $NN = 250$.

[9] The MFD approach can be effectively used to model the global component of complex systems such as the solar wind-magnetosphere coupling. The phase portrait for the magnetosphere in the three dimensional space spanned by the first three principal components of $vB_S - AL$ time series is shown in Figure 2. The technique used earlier [*Sitnov et*

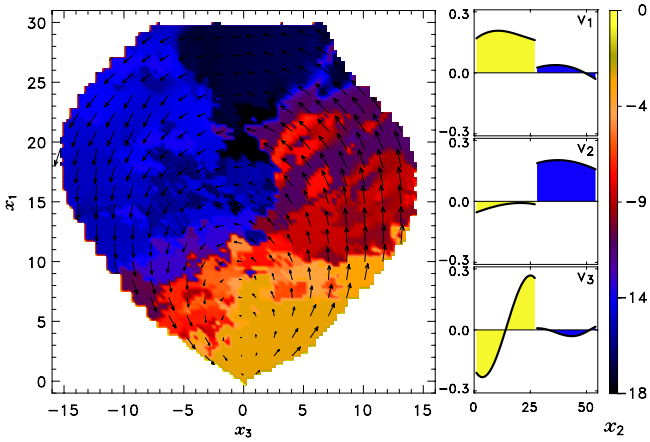

Figure 2. Left panel: phase portrait of the global features of solar wind - magnetosphere coupling during substorms; right panel: first three principal components of $vB_S - AL$ time series.

al., 2000, 2001] for such studies involved cumbersome procedures such as the removal of the hysteresis loops and smoothing of the resultant surface. The MFD approach discussed above resolves these problems by using the most probable states of the nearest neighbors whose number is consistent with the embedding dimension and chosen accuracy. The surface is shown in the $x_1 - x_3$ projection plane defined by the first ($\mathbf{v}_1$) and the third ($\mathbf{v}_3$) principal components. The component x_1 corresponds to the time average value of input (I_t) while x_3 corresponds to its average time derivative [*Sitnov et al.*, 2001]. The projection x_2 of the data on the $\mathbf{v}_2$ direction, which corresponds to the time average value of the output (O_t), is color coded. The evolution of the system along this surface is shown by the two-dimensional velocity field. The substorm cycles are confined to a surface which is broadly two-level, and the levels are associated with the growth phase (orange-yellow colors) and the expansion phase (black-blue colors). The recovery phase corresponds to the transition region with blue-orange-yellow color in the lower left quadrant of Figure 2. The typical substorm cycle starts with an increase in the average input x_1 while the average output x_2 is nearly constant or slowly decreasing, i.e. the system is in the growth phase, which may be viewed as the ground state of the system. During this phase the average input rate x_3 first increases and then decreases to small values. Then the output x_2 falls rapidly to negative values at almost constant values of the input and this corresponds to the expansion phase of substorms, which may be viewed as a transition to the excited state. The recovery of the system to its ground state involves an increase of x_2 while the magnitude of x_3 increases to near-zero values.

[10] In the reconstructed phase space the multi-scale features have been eliminated largely due to the averaging process. They appear as fluctuations around the smooth manifold containing the trajectories of averaged system and their statistical properties depend on the state of the system, $\mathbf{x}_t$, characterized by the input as well as the output, and can be described in terms of a conditional probability $P(O_{t+1}|\mathbf{x}_t)$. At each time step the conditional probability can be estimated using the nearest neighbors of the current state, defined in the MFD analysis, as

$$P(O_{t+1}|\mathbf{x}_t) \approx P(O_{k+1}), \mathbf{x}_k \in NN \quad (5)$$

To analyze the nature of multi-scale dynamical features the evolution of conditional probability $P(O_{t+1}|\mathbf{x}_t)$ is calculated in the one and two-dimensional subspaces spanned by $\mathbf{v}_1$ and ($\mathbf{v}_1$, $\mathbf{v}_3$) principal components of $vB_S - AL$ time series respectively. The probability distribution functions $P(O_t, x_1)$ are shown in Figure 3a for different levels of solar wind activity, represented by the blue, red and yellow colors. The marginal distribution $P(O_t)$ for all levels of the solar wind taken together, is the black curve in the back panel of the plot, and has a power-law shape with a break corresponding to $-AL$ ~500 nT. The distribution functions corresponding to the medium (red) and high (yellow) activities have distinct maxima and thus do not exhibit multi-scale behavior. On the other hand, the distribution function corresponding to the low solar wind activity has a structure similar to the multi-scale marginal distribution. However, if the input space is expanded from one to two dimensions, then the multi-scale functions $P(O_t|x_1)$ break into a number of distribution functions $P(O_t|x_1, x_3)$ with pronounced peaks whose width and position depend on both the input parameters (x_1, x_3) (Figure 3b). With an increase in the phase space dimension the width of the corresponding distribution functions decreases until it saturates at the mean-field dimension. This indicates that a large portion of the multi-scale distribution of AL is directly induced by the similar properties of the solar wind driver rather than being a result of the inherent complexity of magnetospheric dynamics.

[11] The strong influence of the solar wind driver on the multi-scale properties of the system provides a new understanding of the magnetosphere and forms the basis for a

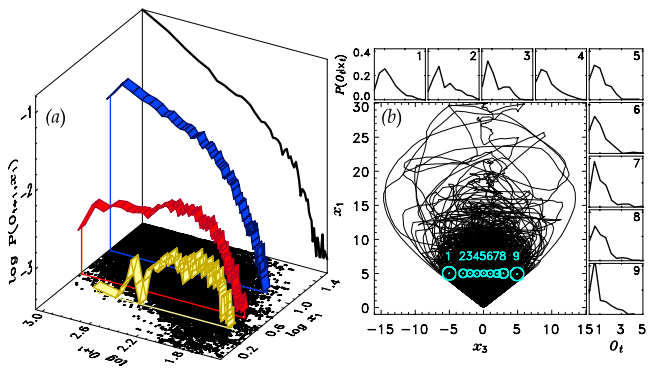

Figure 3. Conditional probabilities of AL as a function of solar wind conditions. (a) $P(O_t, x_1)$: The yellow, red and blue curves correspond to strong ($vB_S > 9$ mV), medium ($0.6 < vB_S < 9$ mV) and low ($vB_S < 0.6$ mV) solar wind activity levels, respectively. The floor shows all point in the database corresponding to the marginal probability distribution function shown in the back panel. (b) $P(O_t|x_1, x_3)$ computed for the points at the centers of the blue circles along the value of x_1 corresponding to the low solar wind activity (blue curve in panel (a)). The circles indicate the clusters of equal number of nearest neighbors that yield the conditional probability functions.

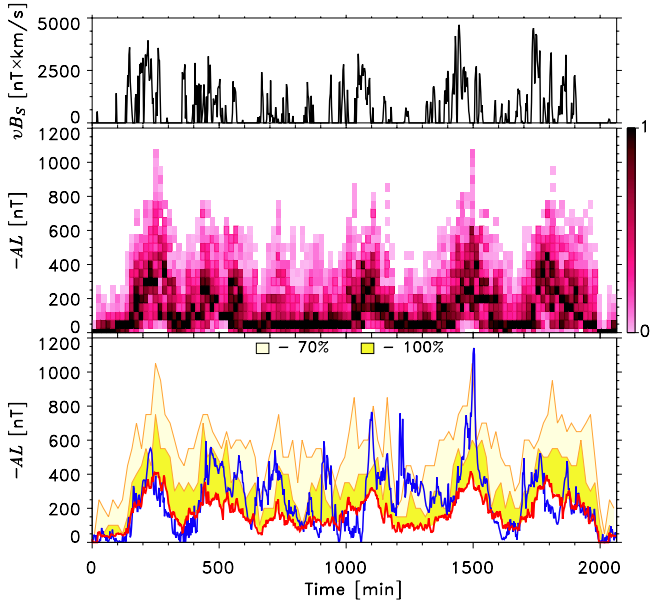

Figure 4. Long-term predictions of *AL* index for the 29th interval of *Bargatze et al* [1985] database. Upper panel: solar wind vB_S data. Middle panel: Probability $P(O_{t+1}|\mathbf{x}_t)$ of *AL* computed with $NN = 50$; $\mathbf{x}_t$ is calculated with the mean-field dimension $D = 5$. Bottom panel: the actual *AL* data (blue), the mean-field prediction (red); contours of probability $P(O_{t+1} > O^{mf}_{t+1}|\mathbf{x}_t)$ of the *AL* deviation from the mean-field model output(yellow shades).

new approach to data-derived modeling. The global behavior can be described by a low-dimensional dynamical model (equation (3)) based on the mean-field concept and the high-dimensional multi-scale features on the other hand are described in terms of conditional probabilities (equation (5)). The predictions from a model with this combination of dynamical and probabilistic descriptions are shown in Figure 4. The *AL* data is shown in blue in Figure 4 (bottom) and the iterative predictions obtained with the mean-field model are shown in red. The mean-field model effectively reproduces the local average of *AL*, yielding predictions of the average level of substorm activity. It should be noted that once the mean-field dimension is defined following the procedure described above, the prediction process does not need any tuning of parameters, unlike the earlier local-linear techniques [*Vassiliadis et al.*, 1995; *Ukhorskiy et al.*, 2002]. Being regular and low-dimensional this component of *AL* is a manifestation of the global constituent of substorm dynamics. However, due to the inherent averaging the model can not capture the abrupt variations in the data and as a result it underestimates the substorm activity in many cases. Being a result of the multi-scale constituent of *AL* these discrepancies can be described in terms of conditional probabilities (equation (5)), which are shown in Figure 4 (middle). Estimated at each time step, these probabilities are then used to compute the probability $P(O_{t+1} > O^{mf}_{t+1}|\mathbf{x}_t)$ of the deviations from the mean-field prediction, shown in Figure 4 (bottom). The probability density functions are computed at each time step using only those events that correspond to *AL* values greater than the mean-field model output. Thus in Figure 4 (bottom) the deviations are represented by the different shades of yellow above the mean-field curve. The 100% contour includes all deviations from the mean-field prediction, including the sharpest peaks and most of the peaks lie below the 70% contour. Thus the model yields not only the deviations from the predictions of the mean-field model but also their probabilities.

3. Conclusions

[12] The new approach presented here for modeling the solar wind-magnetosphere coupling is based on the recognition that the magnetospheric dynamics are neither clearly low dimensional nor completely random, but exhibit combinations of these two aspects. The modeling based on the mean-field concept yields a low dimensional description and the multi-scale aspects are modeled using conditional probabilities. Such a combined approach yields an improved and effective tool for forecasting space weather.

[13] **Acknowledgments.** The research is supported by NSF grants ATM-0001676, 0119196 and 0318629.

References

Angelopoulos, V., et al. (1999), Evidence for intermittency in Earth's plasma sheet and implications for self-organized criticality, *Phys. Plasmas*, *6, 4161.*

Bargatze, L. F., et al. (1985), Magnetospheric impulse response for many levels of geomagnetic activity, *J. Geophys. Res.*, *90*, 6387.

Broomhead, D. S., and G. P. King (1986), Extracting qualitative dynamics from experimental data, *Physica D*, *20*, 217.

Casdagli, M. (1992), A dynamical approach to modeling inpt-output systems, in *Nonlinear Modeling and Forecasting*, edited by M. Casdagli and S. Eubank, p. 265, Addison-Wesley-Longman, Reading, Mass.

Consolini, G. (1997), Sandpile cellular automata and magnetospheric dynamics, in "*Cosmic Physics in the Year 2000*", vol. 58, edited by S. Aiello et al., Soc. Ital. di Fis., Bologna.

Kennel, M. (1992), Determining embedding dimension for phase space reconstruction using a geometrical construction, *Phys. Rev. A*, *45*, 3403.

Lui, A. T. Y., et al. (2000), Is the dynamic magnetosphere an avalanching system?, *Geophys. Res. Lett.*, *27*, 911.

Ohtani, S., et al. (1985), Magnetic fluctuations associated with tail current disruption: Fractal analysis, *J. Geophys. Res.*, *100*, 19,135.

Sitnov, M. I., et al. (2000), Phase transition-like behavior of the magnetosphere during substorms, *J. Geophys. Res.*, *105*, 12,955.

Sitnov, M. I., et al. (2001), Modeling substorm dynamics of the magnetosphere: From self-organization and self-criticality to nonequilibrium phase transitions, *Phys. Rev. E.*, *65*, 016116.

Takalo, J., et al. (1994), Properties of AE data and bicolored noise, *J. Geophys. Res.*, *99*, 13,239.

Tsurutani, B. T., et al. (1990), The nonlinear response of AE to the IMF Bs driver: A spectral break at 5 hours, *Geophys. Res. Lett.*, *17*, 279.

Ukhorskiy, A. Y., M. I. Sitnov, A. S. Sharma, and K. Papadopoulos (2002), Global and multiscale aspects of magnetospheric dynamics in local-linear filters, *J. Geophys. Res.*, *107*(A11), 1369, doi:10.1029/2001JA009160.

Ukhorskiy, A. Y., et al. (2003), Combining global and multi-scale features in a description of the solar wind-magnetosphere coupling, *Ann. Geophys.*, *21*, 1913.

Vassiliadis, D., et al. (1995), A description of the solar wind-magnetosphere coupling based on nonlinear filters, *J. Geophys. Res.*, *100*, 3495.

Vespignani, A., and S. Zapperi (1998), How self-organized criticality works: A unified mean-field picture, *Phys. Rev. E*, *57*, 6345.

K. Papadopoulos, A. S. Sharma, and M. I. Sitnov, Department of Astronomy, University of Maryland, College Park, MD 20742-3921, USA.

A. Y. Ukhorskiy, Applied Physics Laboratory, Johns Hopkins University, Johns Hopkins Road, Laurel, MD 20723-6099, USA. (aleksandr.ukhorskiy@jhuapl.edu)